Influence of Processing Conditions on the Morphological and Mechanical Properties of Compatibilized PP/LCP Blends

Susana Filipe,[1,2*] João Manuel Maia,[1] Catarina Rosa Leal,[3,4] Maria Teresa Cidade[2]

[1]*Polymer Engineering Department, University of Minho, Campus de Azurém, 4800-058 Guimarães, Portugal*
[2]*Materials Science Department and CENIMAT, New University of Lisbon, Campus da Caparica, 2829-516 Caparica, Portugal*
[3]*ISEL, Polytechnical Institut of Lisbon, Scientific Area of Physics, Rua Conselheiro Emídio Navarro,1,1949-014 Lisboa, Portugal*
[4]*C.F.M.C.-Lisbon University, Av. Prof. Gama Pinto 2, P-1649-003 Lisboa, Portugal*

Received 7 July 2006; accepted 23 February 2007
DOI 10.1002/app.26412
Published online 23 April 2007 in Wiley InterScience (www.interscience.wiley.com).

ABSTRACT: The main aim of this work is to study the influence of the application of different processing conditions on the morphological and mechanical properties of thermoplastic/LCP blends, in which the viscosity ratios are inferior to unity and decrease with increasing temperature. The way the microstructure evolves along the extruder determines the final morphology and thus, the mechanical performance of the systems. In the present case, the mechanical properties are related with the degree of fibrillation in the final composites. The best degree of fibrillation was obtained for low screw speeds and temperatures and for intermediate outputs. The use of high screw speeds and processing temperatures results in a decrease of the viscosity ratio, in the former case via an increase in the viscous dissipation, at the regions of higher shear rates (kneading-elements). The application of a lower processing temperature is advantageous for deformation, break-up, and fibrillar formation because of the higher viscosity ratios and higher shear stresses involved. © 2007 Wiley Periodicals, Inc. J Appl Polym Sci 105: 1521–1532, 2007

Key words: liquid crystalline polymers; thermoplastic; blends; processing conditions; isotactic polyproylene

INTRODUCTION

The importance of intermeshing corotating twin-screw extruders in blending processes is clearly recognized, considerable agreement existing about their efficiency in terms of both distributive and dispersive mixing.[1] In these extruders a relatively uniform shear rate distribution is provided along the conveying screw sections and the use of kneading blocks and reverse-conveying elements improves the mixing capabilities.[1] The geometrical properties of the barrel and screw as well as the processing conditions can be changed to optimize the mixing processes.[2,3]

In what concerns blends of immiscible polymers, many studies have been performed to quantify the degree of break-up, coalescence, and deformation of dispersed phase particles at the different stages of the extrusion process.[4–11] Most of these works were performed for noncompatibilized systems but there are some exceptions, like those of Majumdar et al.[11] and Nishio et al.,[12] in which the attention was focused on compatibilized systems.

The extruder used in this work has been widely used before to monitor the evolution of both chemistry and morphology on several systems. Some few examples, are the work done by Machado et al.[13] on blends of polyamide-6-ethylene propylene rubber (PA-6-EPM) and styrene-maleic anhydride (SMA), the study of the evolution of peroxide-induced thermomechanical degradation of PP along the extruder length (Machado et al.[14]) and the evaluation of morphological, rheological, and chemical properties along the extruder length for different systems discussed by Covas et al.[15,16,17] and Machado et al.[18] It is important to point out that this extruder possesses a special home-built collecting device system,[14] which allows the removal of samples (with 2–3 g), in the regions were the highest physical changes are expected, i.e., left-handed screw elements and kneading blocks, without significant disturbance of the flow inside the extruder, and in a very short-time (less than 3 s). The samples removed by this system, are immediately quenched in liquid nitrogen, so that the morphology developed inside the extruder is essentially preserved. In addition to the

Correspondence to: M. T. Cidade (mtc@fct.unl.pt).
**Present address*: Borealis Polyolefine GmbH, Sankt Peter Strasse 25, 4021 Linz, Austria.
Contract grant sponsor: Science and Technology Foundation (Portugal); contract grant number: POCTI/CTM/32,658/99.

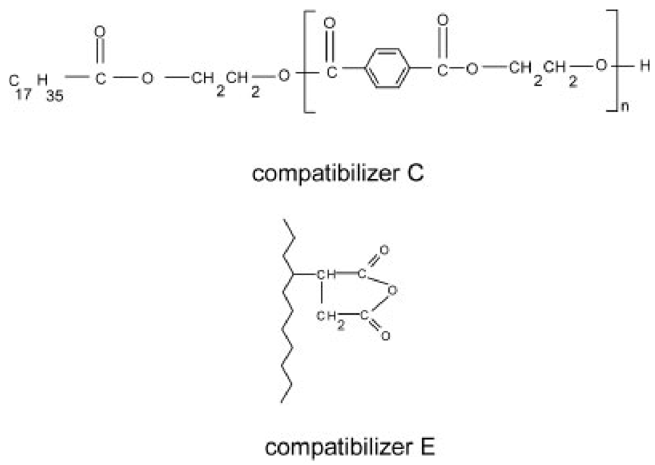

Figure 1 Chemical structures of compatibilizers C and E.

morphological analysis, through the use of this system it is also possible to monitor the evolution of temperature (via a fast thermocouple), study the evolution of the rheological properties during processing (by means of on-line rheometry[14,17]), and analyze the chemical conversion (by analyzing the samples collected at the different locations inside the extruder[18]).

The influence of different LCP contents, as well as different compatibilizers and compatibilizer contents on the evolution of both rheological and morphological properties, as well as the mechanical properties of liquid crystalline and thermoplastic blends (with Rodrun LC3000 and polypropylene), for fixed processing conditions (220°C, 150 rpm and 4 kg/h), was already reported elsewhere.[8–10] The composition of the system affects dramatically the morphological behavior, e.g., the use of an efficient compatibilizer results in the formation of a morphology with a more uniform distribution and smaller average droplet diameters than is the case for systems with low-efficiency compatibilization and noncompatibilized blends.[9] The rheological properties under nonlinear conditions (Fourier Transform Rheology) were shown to be highly sensitive to the morphology developed along the extruder length.[8,9] The nonlinear character, expressed by means of the intensity of the third harmonic over the fundamental one, $I(3\omega_1)/I(\omega_1)$, was higher at the beginning of the extrusion process, which was associated with the presence of LCP droplets with higher average diameters, and thus, easier deformation.[8,9] Furthermore, a decrease of the nonlinear character along the extruder length was observed, which was in accordance with a progressive decrease of the LCP droplet diameters and increase of the orientation, leading at a final stage, at the die exit, to a fibrillar morphology (which shows the lowest nonlinear character among all the samples collected along the extruder length).[8,9]

Even though several articles deal with the mechanical properties of compatibilized thermoplastic/LCP blends, as far as the authors are aware, none of them presented correlations between the degree of fibrillation and the evolution of the morphology along the extruder, which is a consequence of the processing conditions. Thus, in addition to improving the mechanical properties of a PP/Rodrun LC3000 blend and studying the influence of the processing conditions on its mechanical properties, the aim of the present article is to contribute to bridge this gap in knowledge by using the aforementioned extruder with the special sampling devices to establish correlations between the evolution of the morphology along the extruder and the degree of fibrillation (and consequently the mechanical strength).

EXPERIMENTAL

Materials

Blends of polypropylene (Stamylan P 12E62, from DSM) and Rodrun LC3000 (from Unitika) were performed by extrusion. The thermoplastic used for the preparation of the blends is an isotatic polymer with a weight-average molecular weight ($\overline{M}_w$) of 1,200,000 g/mol (obtained by GPC) and a melt flow index of 0.8 g/10 min (at 230°C and for 21.6*N*). The liquid crystalline polymer is an aleatory copolyester of 60% mol of *p*-hydroxybenzoic acid and 40% mol of polyethylene terephthalate (PET). The molecular weight for the LCP was not obtainable, since no solvent was found to dissolve Rodrun LC3000.

To improve the adhesion between the pure components and thus the mechanical properties, two different compatibilisers were used. The first has a thermoplastic nature and was synthesized in the framework of this work[19] and the second possesses an elastomeric nature and is commercially available with the trade name Exxelor VA 18,020 (supplied by Exxon Mobil Chemical); their chemical structures are depicted in Figure 1. For the sake of coherence with previous works,[9,10,19,20] it was decided to keep the denomination of each compatibilizer, the former being labeled compatibilizer C and the latter compatibilizer E. These were those that demonstrated to be more efficient on the compatibilization process of the Rodrun LC3000 and PP blends under study.[20] The

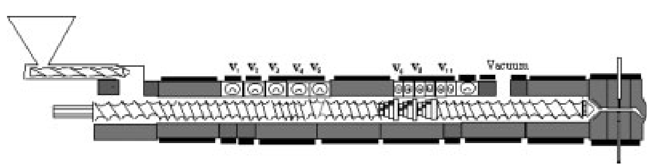

Figure 2 Screw and cylinder profiles used for the preparation of LCP/TP blends.

TABLE I
Processing Conditions Used for the Optimization Process

Processing conditions	Cond. 1	Cond. 2	Cond. 3	Cond. 4	Cond. 5	Cond. 6
Temperature (°C)	220	240	220	220	220	220
Screw speed (rpm)	150	150	100	200	150	150
Output (kg/h)	4	4	4	4	2	8

optimum compatibilizer and LCP contents (2 wt % of compatibilizer C and 4 wt % of compatibilizer E, in both cases with 10 wt % LCP) were determined in a previous work.[10]

Extrusion conditions

An intermeshing corotating twin-screw extruder from Leistritz, model LSM 30.34 was used for the preparation of the blends (Fig. 2). The screw used is constituted by a conveying region, followed by a reverse-conveying element. After this, the screw is constituted by a second conveying region, which is followed by eleven staggering kneading blocks (with a staggering angle of −60°) and by a final group of conveying elements.

The cylinder and screw configurations were defined in such a way that the valves are placed in the zones of the screw in which the highest positive pressures exists (left-handed elements and kneading blocks). Thus, it is possible to collect samples in those locations where the highest morphological changes are expected to occur. In this configuration (Fig. 2) a group of six small valves was placed near the region with the kneading blocks. This procedure was made to evaluate the way how the morphology develops, before, during and after the kneading blocks region.

The extrusion conditions were those shown in Table I and were designed to allow the study of the influence of screw speed, temperature and output on the morphological and mechanical properties.

Before extrusion all the materials were dried in an oven at 90°C for 24 h. Such a procedure does not lead to any thermal degradation, as confirmed via time sweep measurements performed for several hours, at much higher temperatures (220 and 240 °C). As usual, the final rod-shaped extrudates (the die diameter was 1 mm) were immediately quenched in a water bath and subsequently pelletised. Samples were collected at the different positions along the extruder. As already described, the samples removed by this system were also immediately quenched in liquid nitrogen to preserve the morphology, as developed inside the extruder.

Injection molding conditions

Once again, and similarly to the procedure followed for the extrusion process, all the blends were dried in an oven at 90°C for 24 h before injection molding. Tensile specimens (dogbone-shaped) with 60 × 4 × 2 mm (length × width × thickness) were produced by injection molding using an injection molding machine ENGEL model ES200/45 HL-V. The temperature profile used for this purpose was 170, 190, and 200°C, for the first, second, and third zones of the barrel, respectively. The nozzle temperature was

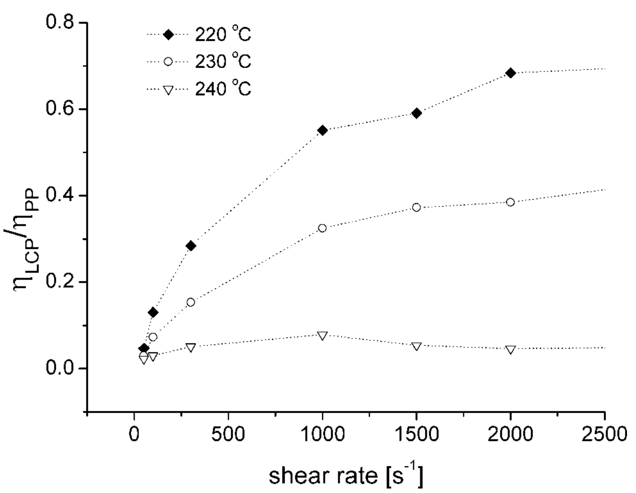

Figure 3 Viscosity ratio of matrix and dispersed phase at different temperatures.

TABLE IIa
Average Diameters (μm) Along the Extruder Length for Blends with 2 wt % Compatibilizer C

Processing conditions	v4	v6	v8
Q^a (kg/h)			
2	8.70	6.80	5.30
4	8.67	5.87	6.15
8	–	5.86	3.84
N^b (rpm)			
100	6.12	8.96	4.53
150	8.67	5.87	6.15
200	8.46	–	7.70
T^c (°C)			
220	8.67	5.87	6.15
240	–	8.57	5.65

[a] $T = 220°C$, $N = 150$ rpm.
[b] $T = 220°C$, $Q = 4$ kg/h.
[c] $Q = 4$ kg/h, $N = 150$ rpm.

TABLE IIb
Average Diameters (μm) Along the Extruder Length for Blends with 4 wt % Compatibilizer E

Processing conditions	v4	v6	v8
Q^a (kg/h)			
2	5.00	6.72	5.53
4	12.20	6.59	4.53
8	7.45	5.14	6.96
N^b(rpm)			
100	8.04	5.67	5.63
150	12.20	6.59	4.53
200	8.70	6.80	4.93
T^c (°C)			
220	12.20	6.59	4.53
240	7.25	6.39	7.23

[a] $T = 220°C$, $N = 150$ rpm.
[b] $T = 220°C$, $Q = 4$ kg/h.
[c] $Q = 4$ kg/h, $N = 150$ rpm.

set at 210°C and the mold temperature used was 30°C.

By keeping the injection molding temperature relatively low and the injection conditions as mild as possible, it was hoped that the inevitable changes that occur in the morphology of the samples due to an extra processing cycle would not eliminate completely (but only mitigate) existing differences in morphology at the end of the extrusion process, i.e., it was hoped that there will not be a complete relaxation of the dispersed phase, the LCP. This expectation was confirmed when scanning electron miscroscopy (SEM) was performed on injection-molded samples and the differences in fibrillation, observed with the samples prepared with different processing conditions, were still clearly visible, as will be shown later.

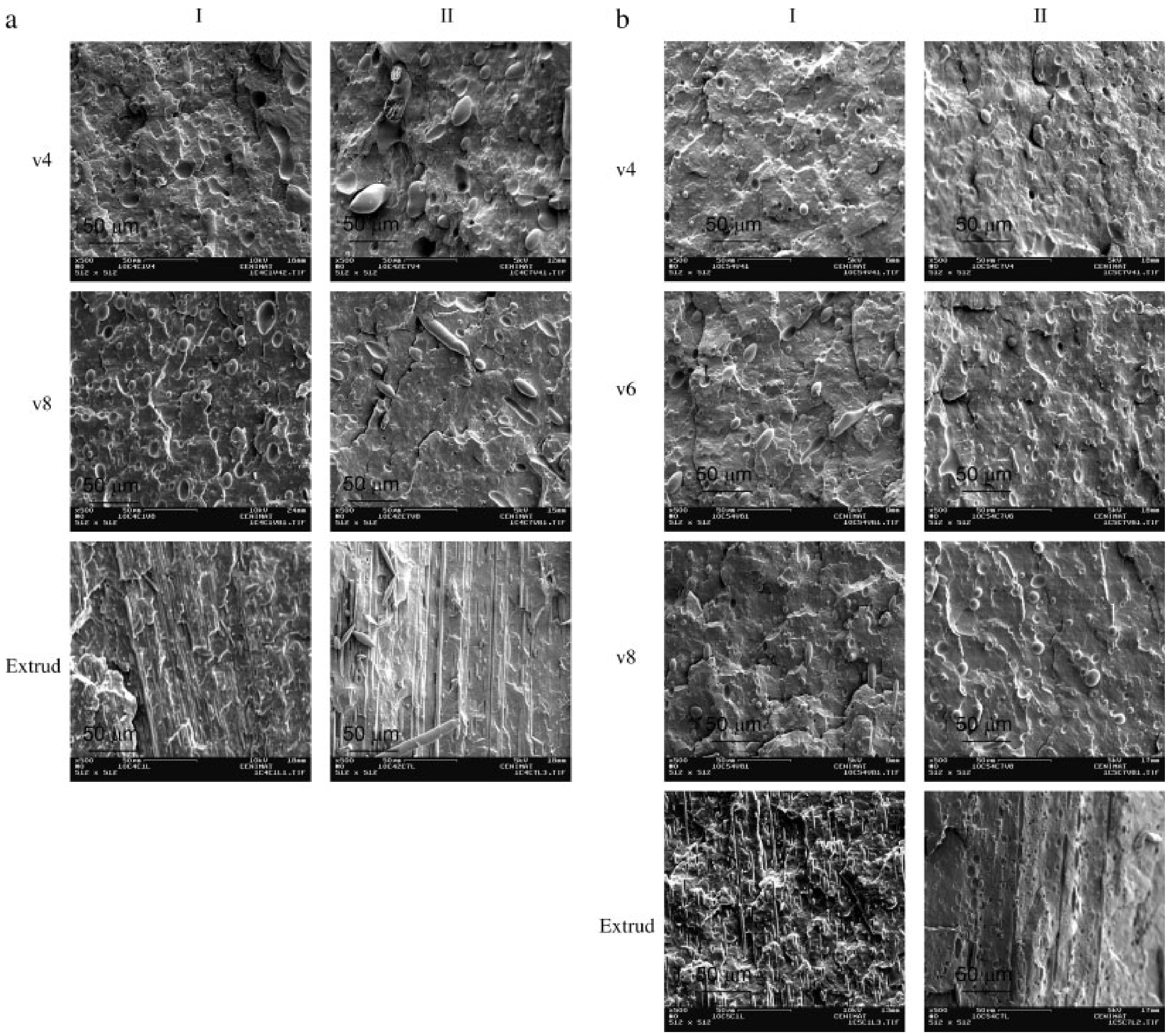

Figure 4 SEM images for blends with 10 wt % LCP and 2 wt % compatibilizer C (a) and 4 wt % compatibilizer E (b), processed at 220°C (I) and 240°C (II)-Magnification of ×500.

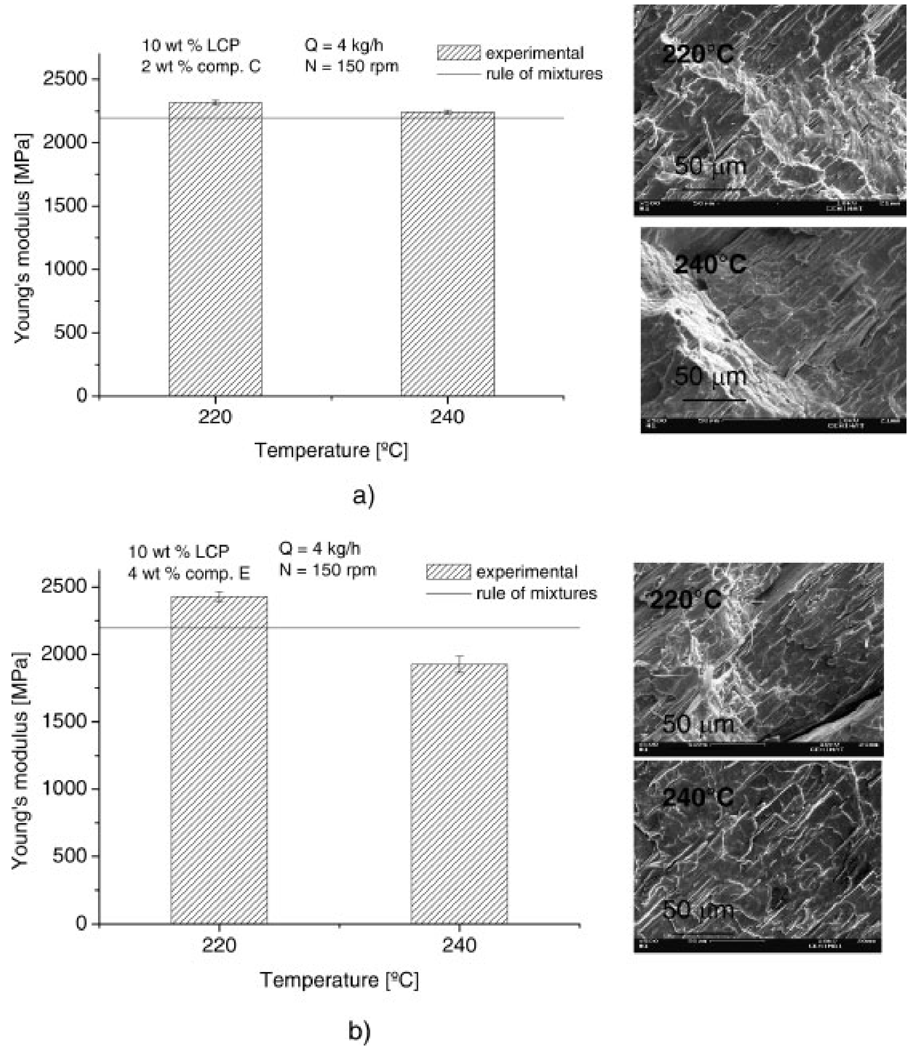

Figure 5 SEM micrographs of longitudinal cuts of the dog-bone specimens and corresponding Young's modulus for blends processed at 220 and 240°C, with 10 wt % LCP and 2 wt % compatibilizer C (a) and 4 wt % compatibilizer E (b).

Morphological characterization and image analysis

All the blends were analyzed by SEM using a Zeiss DSM 962 apparatus. All the samples were fractured in liquid nitrogen, the final extrudates being fractured longitudinally instead of the more common transversal fracture, because this allowed for a better observation of the fibrils. Apart from the observation of samples collected along the extruder length and of the extrudates, additional SEM investigation was performed on the dog-bone specimens used for the mechanical characterization. Before being examined by SEM all the samples were previously coated with gold, using a POLARON SC502 SEM and were examined at an accelerating voltage of 10 kV. For the analysis of the SEM images and particularly for the determination of the particle size distribution and average diameters, we resorted to the UTHSCSA Image Tool. The area (A) was determined by the use

TABLE IIIa
Temperature Profiles (°C) Along the Extruder Length for Blends with 2 wt % Compatibilizer C

Processing conditions	Position in the extruder			
	v4	v6	v8	Extrudate
Q^a (kg/h)				
2	232.1	233.3	235.4	237.3
4	227.2	230.1	231.4	237.1
8	226.1	227.4	228.2	227.7
N^b (rpm)				
100	226.4	226.7	231.0	233.9
150	227.2	230.1	231.4	237.1
200	227.5	234.7	235.4	238.2
T^c (°C)				
220	227.2	230.1	231.4	237.1
240	244.1	245.9	246.2	248.1

[a] $T = 220°C$, $N = 150$ rpm.
[b] $T = 220°C$, $Q = 4$ kg/h.
[c] $Q = 4$ kg/h, $N = 150$ rpm.

TABLE IIIb
Temperature Profiles (°C) Along the Extruder Length for Blends with 4 wt % Compatibilizer E

	Position in the extruder			
Processing conditions	v4	v6	v8	Extrudate
Q^a (kg/h)				
2	232.9	233.4	237.1	238.1
4	230.1	231.8	236.3	237.2
8	228.1	223.6	231.1	233.9
N^b (rpm)				
100	228.5	229.1	233.4	235.1
150	230.1	231.8	236.3	238.4
200	232.4	229.4	237.1	240.2
T^c (°C)				
220	230.1	231.8	236.3	240.2
240	245.4	247.1	248.4	248.8

[a] $T = 220°C$, $N = 150$ rpm.
[b] $T = 220°C$, $Q = 4$ kg/h.
[c] $Q = 4$ kg/h, $N = 150$ rpm.

of ellipses and was used afterwards to determine the equivalent diameter (d), by using the following equation:

$$d = \sqrt{\frac{4}{\pi} A} \quad (1)$$

For a number of particles, n, the average diameter (d_a) was calculated by using:

$$d_a = \frac{\sum_i d_i}{n} \quad (2)$$

Mechanical characterization

The tensile properties were tested using an Instron Universal Tester Machine model 1.16 at room temperature. A cross-head speed of 5 mm/min and

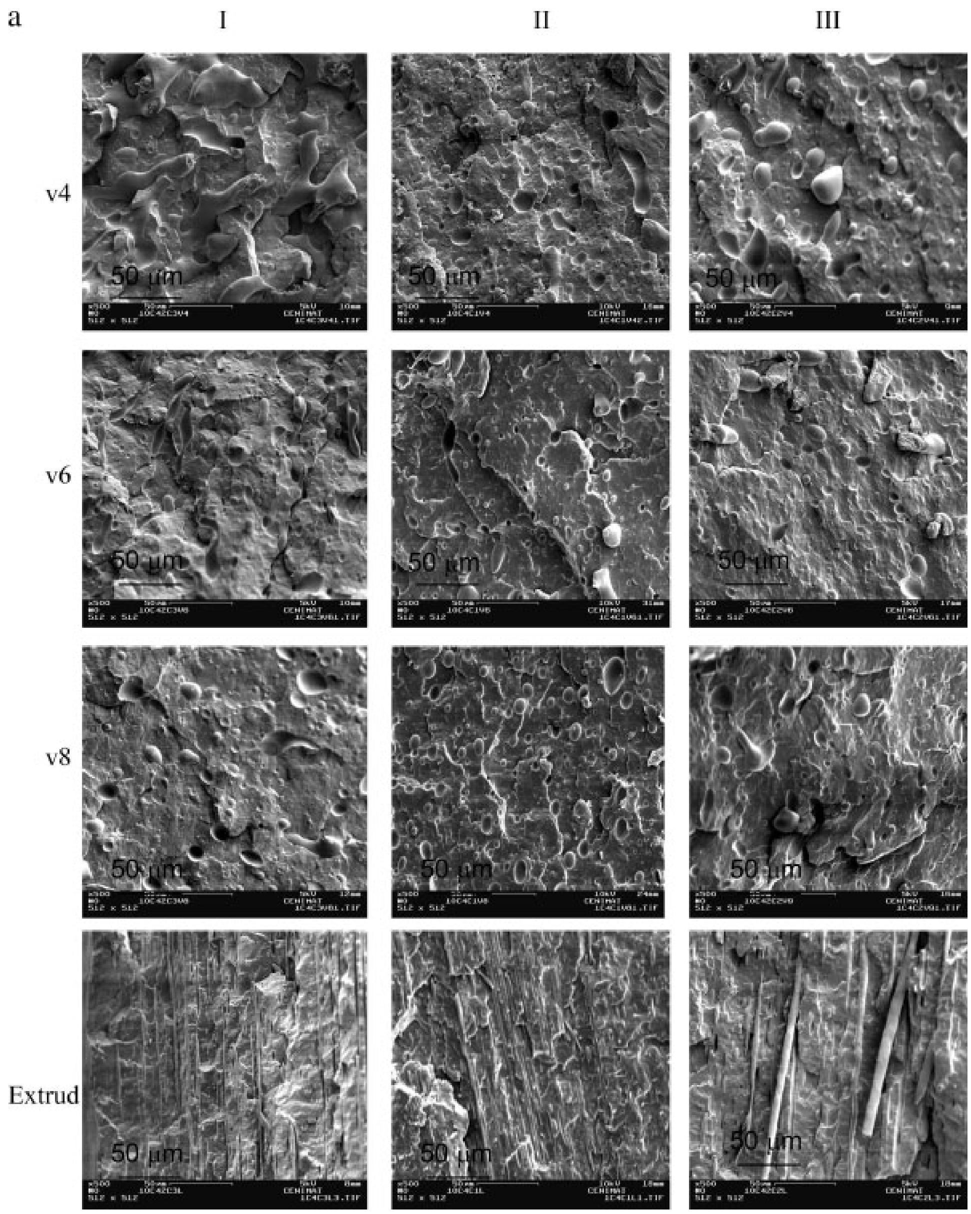

Figure 6 SEM images for blends with 10 wt % LCP and 2 wt % compatibilizer C (a) and 4 wt % compatibiliser E (b) processed at 100 rpm (I), 150 rpm (II) and 200 rpm(III)-Magnification of ×500.

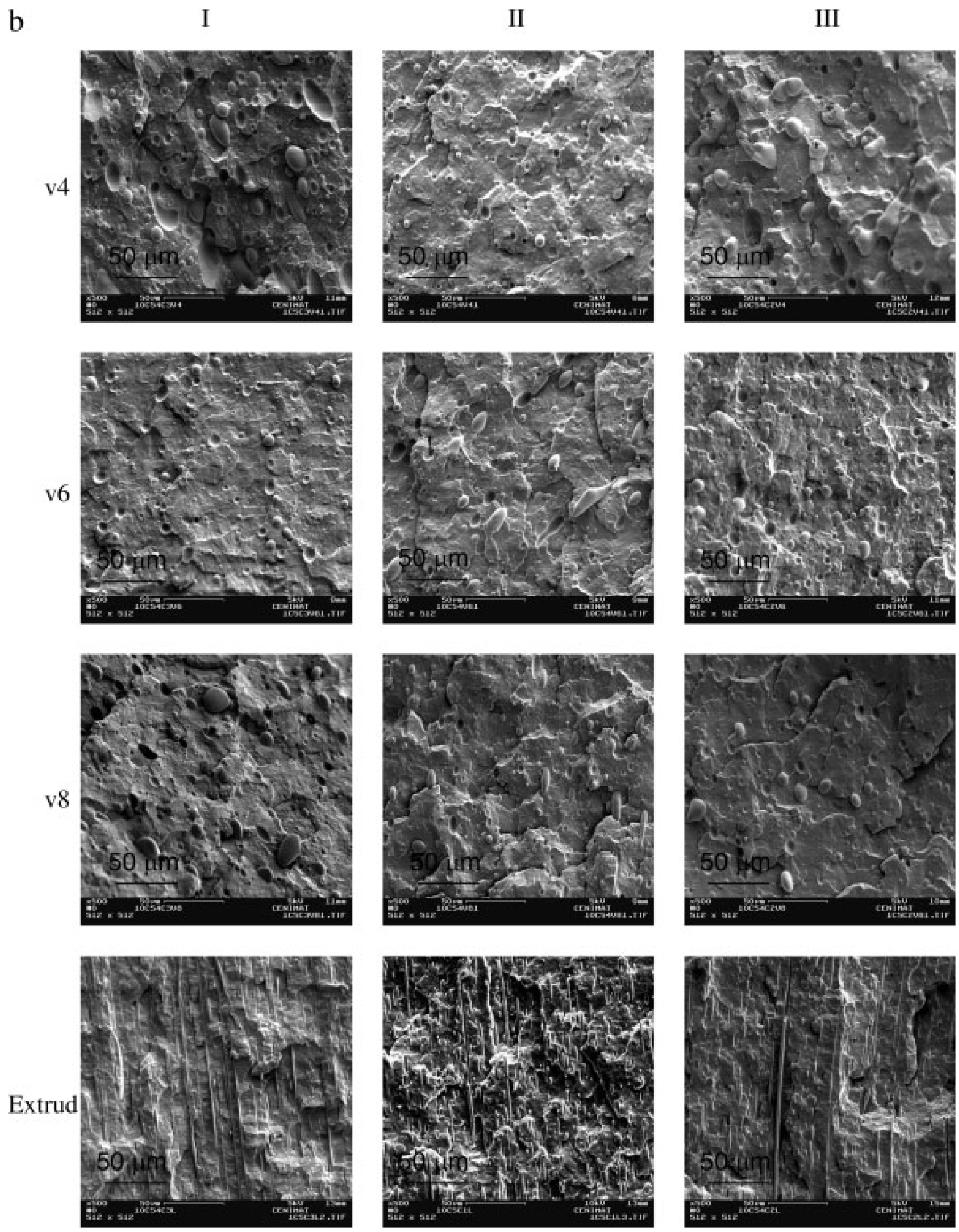

Figure 6 (*Continued from the previous page*)

a load cell of 50 kN were used. An extensometer (model Instron 2630-100) was used for these measurements. The mean and the standard deviation for the different tensile properties were calculated from five specimens.

RESULTS

Influence of processing temperature

Independently of the compatibilizer used, C or E, an increase of the temperature results in a decrease of the viscosity of both components and in a lower viscosity ratio since the LCP is more influenced by the temperature than the PP (Fig. 3). In terms of average droplet size [Tables II(a,b)], at 220°C there is a marked decrease from the reverse conveying area to the beginning of the kneading section, for both compatibilizers, and a relative stabilization (with a possible slight tendency to increasingly smaller sizes in the case of compatibilizer E) thereafter inside the extruder. Increasing the processing temperature to 240°C leads, in the case of compatibilizer E, to smaller changes in average particle size along the extruder. In the case of compatibilizer C, the particle size seems to decrease along the kneading section.

Morphologically, it is quite clear that the dispersed droplets structures that develop inside the extruder turn into a fibrillar one at the die exit and that the increase in processing temperature is clearly detri-

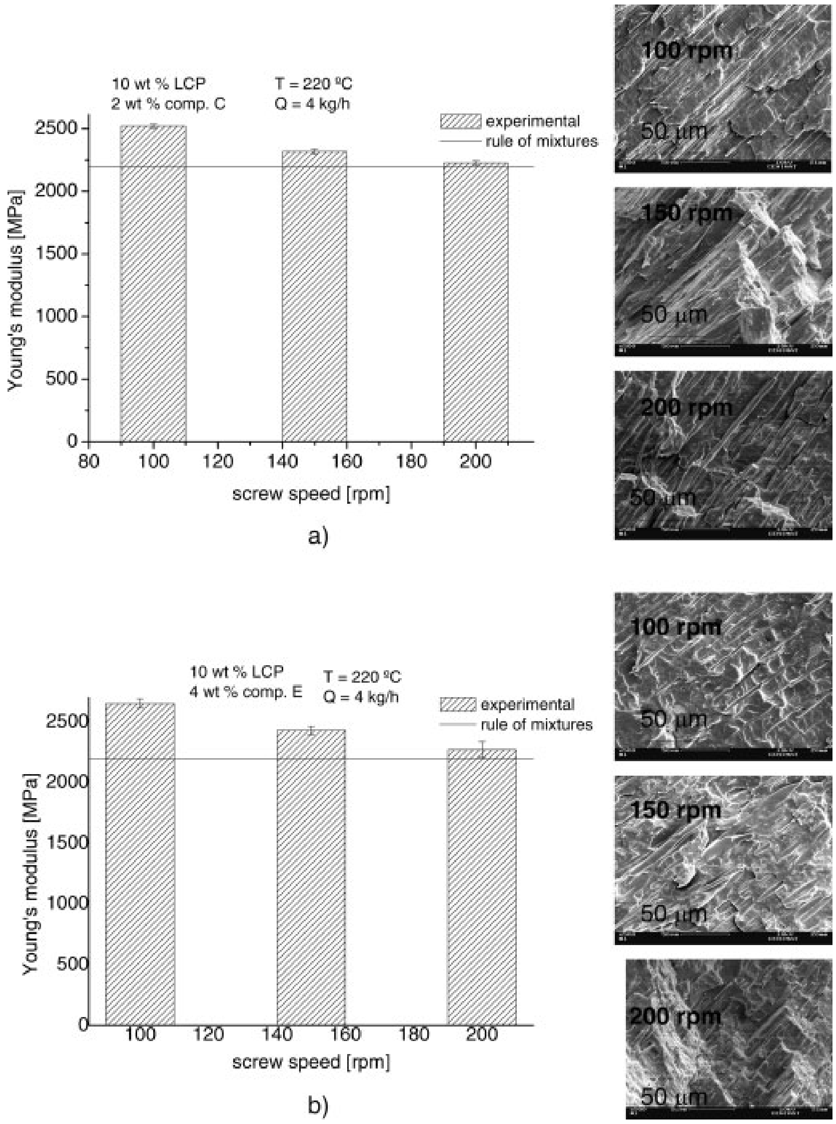

Figure 7 SEM micrographs of longitudinal cuts of the dog-bone specimens and corresponding Young's modulus for blends processed at 100, 150, and 200 rpm, with 10 wt % LCP and 2 wt % compatibilizer C (a) and 4 wt % compatibilizer E (b).

mental to the formation of the fibrils, again due to the lower viscosity ratio (Fig. 4), which, in turn, leads to worse mechanical properties. This is especially so in the case of the blend with compatibilizer E, where the decrease in modulus, even after injection molding, is still superior to 25% (Fig. 5). When 240°C is used as processing temperature the majority of the LCP structures in the extrudate remain in the form of droplets for this blend, whereas for the blend with compatibiliser C fibrils can still be seen, although they are thicker than those fibrils obtained at 220°C (Fig. 4). Although, less evident, the morphology of the dog-bone specimens used for the mechanical testing also indicates a better fibrillation for the blends processed at 220°C (Fig. 5). The increase of the temperature had also repercussions in the elongation at break. The materials processed at a higher temperature, 240°C showed a much ductile behavior, thus presenting higher elongation at break than those extruded at 220°C, as expected.

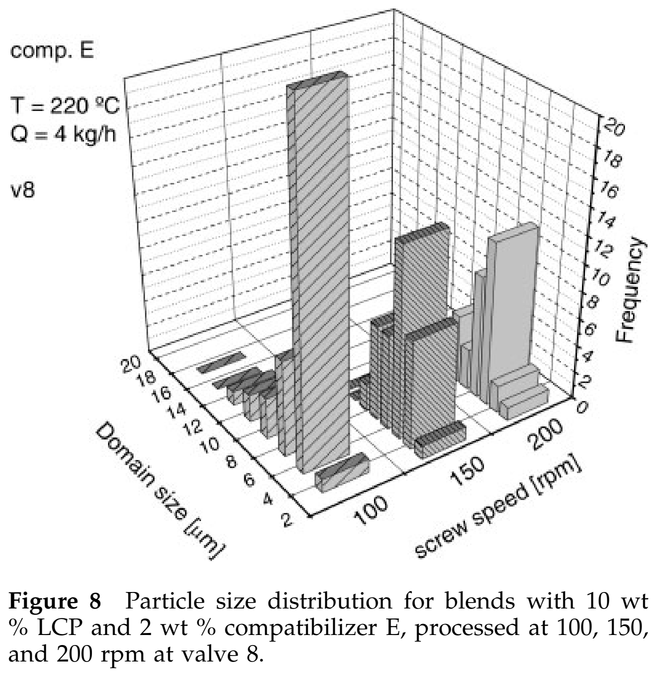

Figure 8 Particle size distribution for blends with 10 wt % LCP and 2 wt % compatibilizer E, processed at 100, 150, and 200 rpm at valve 8.

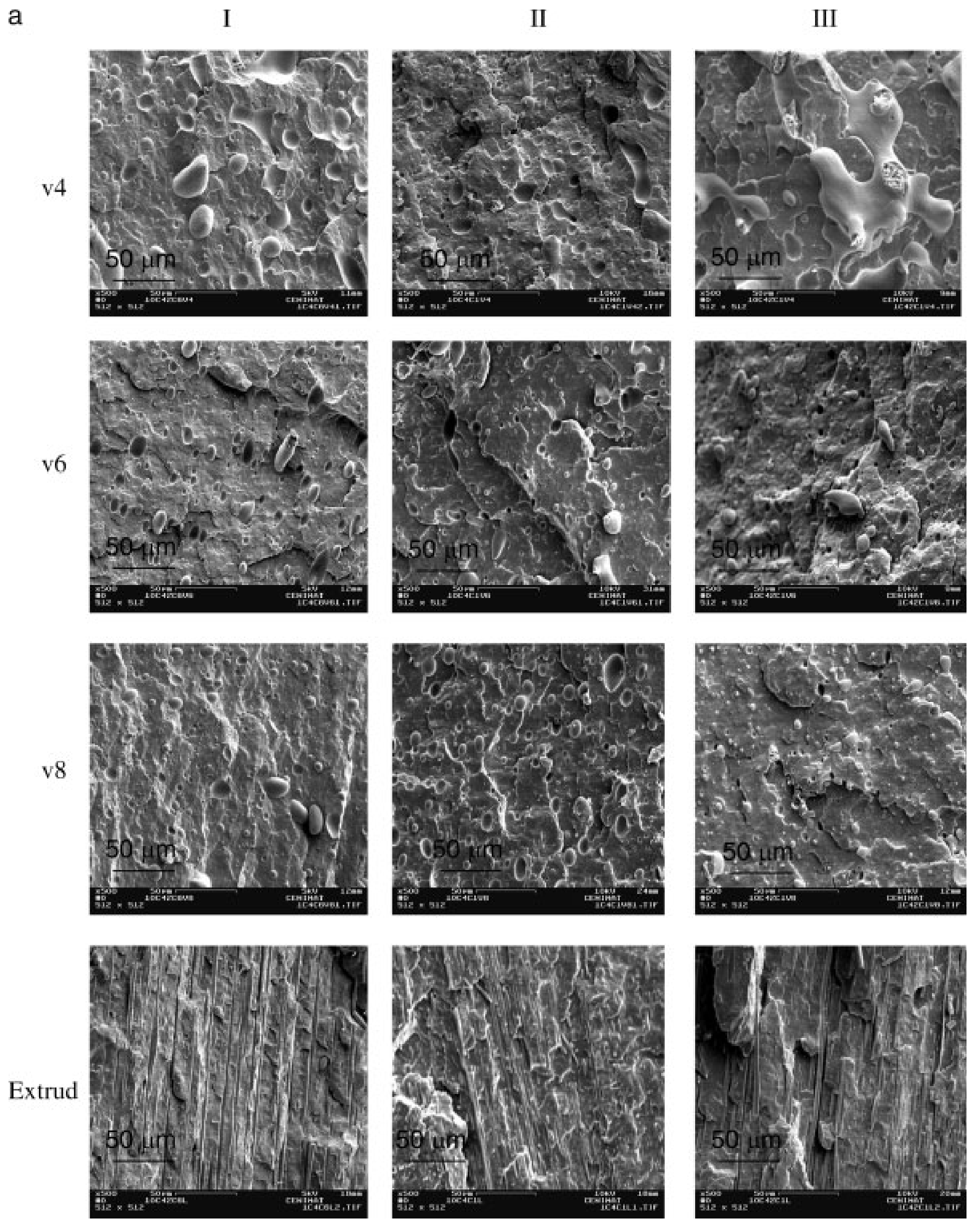

Figure 9 SEM images for blends with 10 wt % LCP and 2 wt % compatibilizer C (a) and 4 wt % compatibilizer E (b), processed at 2 kg/h (I), 4 kg/h (II) and 8 kg/h (III)-Magnification of ×500.

In terms of true melt temperature, it is clear that the viscous dissipation is higher for 220°C than for 240°C (Table III). When the temperature was set at 220°C, the temperature measured at the die exit was 7°C and 13.9°C higher than the set temperature, for the blends with compatibilizer C and E, respectively. A similar in nature but smaller increase of the temperature was also found when a set temperature of 240°C was used (Table III).

Influence of screw speed

In what regards the influence of the screw speed, it can be stated that the application of lower screw speeds seems to be beneficial to the fibrillation process, during both extrusion (Fig. 6) and injection molding (Fig. 7) and, thus, to the mechanical properties, independently of the compatibilizer used (Figs. 6 and 7). For compatibilizer C, the application of different screw speeds seems to result in different morphologies at the beginning of the extrusion process (valve 4). When a screw speed of 100 rpm is applied, the LCP remains in the form of big aggregates and a cocontinuous morphology is present, whereas for the higher screw speeds, 150 and 200 rpm, the LCP is present in the form of droplets dispersed along the thermoplastic matrix [Fig. 6(a)]. This was the expected behavior, since, in principle, the higher the screw speed the higher the shear rate, and thus, the higher the degree of mixing in the initial stages of processing. As the material progresses inside the

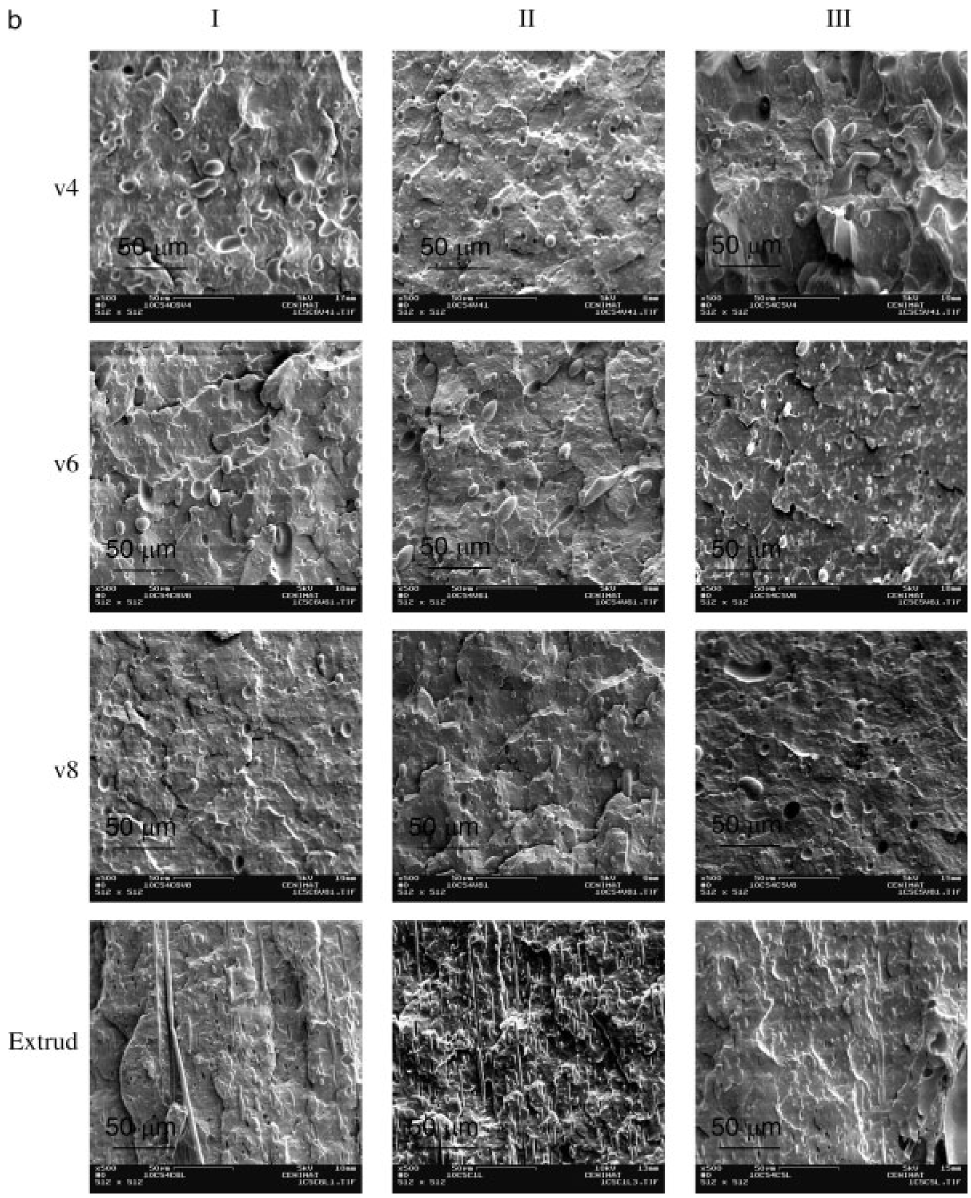

Figure 9 (*Continued from the previous page*)

extruder, it is possible to see that a dispersed droplet-type structure is always present with smaller sized droplets for lower screw speeds; for example, at valve 8, the average diameters are 4.53 for 100 rpm, 6.15 for 150 rpm, and 7.70 for 200 rpm [Table II(a)]. At the die exit, all three sets of screw speeds yield a fibrillar structure but there are significant differences between them; as the screw speed is increased so does the presence of nonfibrillated LCP, i.e., some LCP droplets still remain. These differences have some repercussion in the mechanical properties, even after injection molding, with a slightly decreasing Young's modulus (by about 10% from 100 to 200 rpm), accompanied by a increase of the elongation at break (ductility) with increasing screw speed [Fig. 7(a)].

One strong possibility for the decrease in the fibrillation degree with increasing screw speed is the increase in true melt temperature (with the consequent lower viscosity ratio) with screw speed [Table III(a)] due to increased viscous heating yielded by the increased shear rates. Similar observations have been reported by other authors.[4,12,21–23]

Similarly, for the blend with compatibilizer E it seems that a better dispersion and a higher fibrillar formation at the end of the process occur for the lower screw speeds [Fig. 6(b)]. In the final extrudates both fibrils and droplet-like structures are present for 150 and 200 rpm, while for 100 rpm only fibrils exist. Again, an increase in screw speed results in an augmented viscous heating [Table III(b)] and thus, in a lower viscosity ratio and more difficult droplet

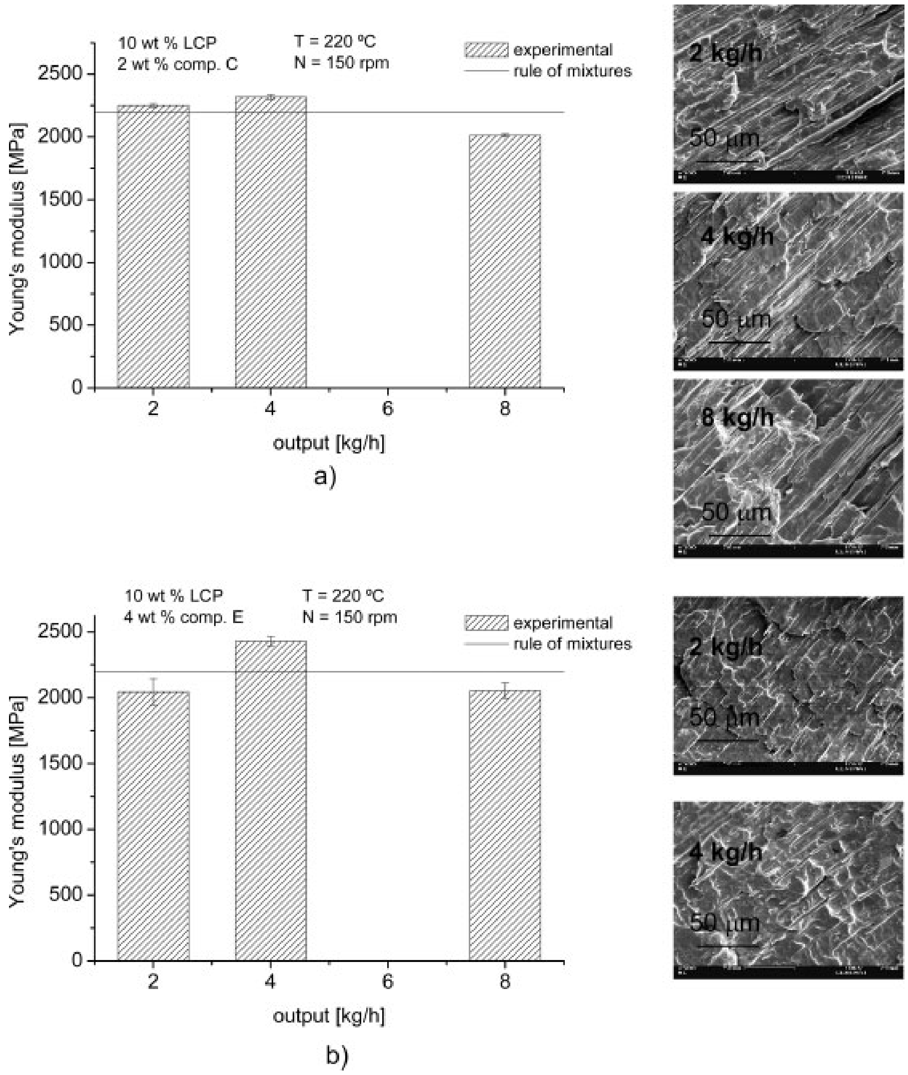

Figure 10 SEM micrographs of longitudinal cuts of the dog-bone specimens and corresponding Young's modulus for blends processed at 2, 4, and 8 kg/h, with 10 wt % LCP and 2 wt % compatibilizer C (a) and 4 wt % compatibilizer E (b).

break-up. The mechanical measurements also revealed that the use of higher screw speeds results in lower Young's modulus [Fig. 7(b)], the total decrease from 100 to 200 rpm being of ∼ 15%.

In terms of droplet size evolution inside the extruder [Table II(b)], for the blends with compatibilizer E it is possible to see that the average size decreases along the extruder for all screw speeds, as expected, but that at valve 8, and in opposition to the blends with compatibilizer C, there are no significant differences in average dimensions. Thus, the reason for the improved fibrillar formation at 100 rpm must be searched for elsewhere. Figure 8 depicts the particle size distribution for the blends processed with compatibilizer E and it is possible to see that it is much narrower at 100 rpm than at 150 or 200 rpm. Thus, although the average sizes are similar, there are more ''big'' droplets at the higher screw speeds that will not be transformed into fibrils in the die.

Influence of output

Contrarily to the previous cases, when the influence of output on the morphology and final mechanical properties of the blends is analyzed, the best results are achieved for intermediate outputs, 4 kg/h, and not at the highest or lowest ones, 8 kg/h and 2 kg/h, respectively. For blends processed with compatibilizer C the maximum increase in Young's modulus between the worst and best cases is ∼ 12% but for those processed with compatibilizer E it is nearly 20% (Fig. 10). Similarly, the application of different throughputs had an effect on the elongation at break for both compatibilized blends. These results are generally consistent with the morphological analysis (Fig. 9) that shows that both the morphology evolution along the extruder and the fibrillar structure of the extrudate are difficult to distinguish for the blends processed with compatibilizer C for 2 and 4 kg/h; for 8 kg/h differences can be observed, with much less fibrillation occurring [Fig. 9(a)]. For the blends processed with compatibilizer E the fibrillar structure of the extrudate is clearly better defined for 4 kg/h [Fig. 9(b)]. From the final morphology of the dogbone specimens, one can state that lower and higher outputs lead to the formation of thicker fibrils, as seen in Figure 10.

The reasons for this behavior are by no means clear and certainly deserve a more careful and exhaustive analysis, but it is feasible that two factors may be competing in this situation:

a. The lower the output, the more effective the heat transfer to the material (for a given screw speed) and the higher the viscous heating, due to the lower degree of filling and consequent higher shear rates. This is confirmed by the analysis of Tables III(a,b), where it is clear that the temperature decreases by up to 7°C from 2 to 8 kg/h. This should lead to a decrease of the degree of fibrillation and mechanical properties with decreasing output.
b. The higher the output, the lower the effective shear rate and the lower the degree of fibrillation. Thus, this mechanism should lead to a decrease of the degree of fibrillation and mechanical properties with increasing output. From the analysis of Figures 8 and 9, it is apparent that the combination of these two competing factors will result in enhanced properties at intermediate outputs.

CONCLUSIONS

The formation of fibrillar structures and thus the mechanical enhancement provided in the direction of the flow are highly dependent on the processing conditions employed, specially screw speed and temperature. The application of different processing conditions affects the way how the morphology evolves and determines the final degree of fibrillation. In particular, when studying the evolution of the morphological properties along the extruder length it is not possible to discard the effects, for example, of viscous dissipation, degree of filling of the screws and residence time.

Although the mechanical properties of the materials were determined for samples submitted to a second processing cycle, and thus eventual differences in the extrudates will have been minimized after the injection molding cycle (although this was performed in the mildest conditions possible), it is still possible to draw some conclusions. For example, it is clear from the present study that some factors, namely higher screw speeds, which may be intuitively believed to improve the degree of dispersive and distributive mixing, may actually have an opposite effect in compatibilized systems, like those studied in this work. Indeed, the dominating factors in achieving high degrees of fibrillation (that, in turn, lead to better mechanical properties) seem to be the droplet size inside the extruder and the thermomechanical conditions that control the effective viscosity ratio. In fact, it seems that when the viscosity ratio is lower than 1 and decreases with increasing temperature, as is the case in these blends, it is advisable to use processing conditions that minimize the effective melt temperature and, thus, maximize droplet break-up inside the extruder.

The authors would like to acknowledge to Prof. Moura Bordado and Miss Ana Paula Duarte for the synthesis of compatibilizer C.

References

1. Utracki, L. A., Ed. Progress in Polymer Science, Two-Phase Polymer Systems; Hanser: Munich, Germany, 1991.
2. Todd, D. B., Ed. Plastics Compoundin; Hanser: Munich, Germany, 1998.
3. Rauwendaal, C. Polymer Extrusion; Hanser: Munich, Germany, 1990.
4. Potente, H.; Bastian, M.; Gehring, A.; Stephan, M. Potschke, P. J Appl Polym Sci 2000, 76, 708.
5. Bordereau, V.; Shi, Z. H.; Utracki, L. A.; Sammut, P.; Carrega, M. Polym Eng Sci 1992, 32, 1846.
6. Boersma, A.; Van Turnhout, J. Polymer 1999, 40, 5023.
7. Sundaraj, U.; Macosko, C. W. Macromolecules 1995, 28, 2647.
8. Filipe, S. Cidade, M. T.; Wilhelm, M.; Maia, J. M.; Polymer 2004, 45, 2367.
9. Filipe, S.; Cidade, M. T.; Wilhelm, M.; Maia, J. M. J Appl Polym Sci 2006, 99, 347.
10. Filipe, S.; Duarte, A.; Leal, C. R.; Menon, A. R. R.; Maia, J. M. Cidade, M. T. J Polym Eng 2006, 26, 511.
11. Majumdar, B.; Paul, D. R.; Oshinski, A. J. Polymer 1997, 38, 1787.
12. Nishio, T.; Suzuki, Y.; Kojima, K.; Kakugo, M. J Polym Eng 1991, 10, 123.
13. Machado, A. V.; Covas, J. A.; Van Duin, M.; J Appl Polym Sci 1999, 71, 135.
14. Machado, A. V.; Maia, J. M.; Canevarolo, S. V.; Covas, J. A.; J Appl Polym Sci 1999, 91, 2711.
15. Covas, J. A.; Carneiro, O. S.; Maia, J. M.; Filipe, S. A.; Machado, A. V. Can J Chem Eng 2002, 80, 1065.
16. Covas, J. A.; Carneiro, O. S.; Costa, P.; Machado, A. V.; Maia, J. M. Plast Rubber Compos 2004, 33, 55.
17. Covas, J. A.; Carneiro, O. S.; Maia, J. M. Int J Polym Mater 2001, 50, 445.
18. Machado, A. V.; Van Duin, M.; Covas, J. A.; Adv Polym Technol 2004, 23, 196.
19. Cidade, M. T.; Filipe, S.; Duarte, A. P.; Bordado, J. C. M. J Appl Polym Sci, to appear.
20. Filipe, S.; Duarte, A.; Leal, C. R.; Maia, J. M.; Cidade, M. T. J Appl Polym Sci 2005, 98, 694.
21. Shi, Z. H.; Utracki, L. A. Polym Eng Sci 1992, 32, 1834.
22. Luciani, A.; Champagne, M. F.; Utracki, L. A. Polym Netw Blend 1996, 6, 41.
23. Carneiro, O. S.; Covas, J. A.; Vergnes, B. J Appl Polym Sci 2000, 78, 1419.